*Korean J. Chem. Eng.*, **29**(5), 657-667 (2012)
DOI: 10.1007/s11814-011-0235-x

# PRSV equation of state parameter modeling through artificial neural network and adaptive network-based fuzzy inference system

**Tahmaseb Hatami*,**, Masoud Rahimi*,†, Hiua Daraei***, Ehsan Heidaryan*, and Ammar Abdulaziz Alsairafi****

*CFD Research Center, Department of Chemical Engineering, Razi University, Kermanshah, Iran
**Faculty of Engineering, Department of Chemical Engineering, University of Kurdistan, Sanandaj, Iran
***Environmental Health Research Center, Kurdistan University of Medical Sciences, Sanandaj, Iran
****Faculty of Mechanical Engineering, College of Engineering and Petroleum, Kuwait University, Kuwait
(*Received 20 April 2011 • accepted 8 September 2011*)

**Abstract**–Two different modeling methods have been proposed to relate the Peng-Robinson-Stryjek-Vera (PRSV) parameter, $\kappa_1$, to some common thermodynamic constants, including critical temperature ($T_c$), critical pressure ($P_c$), acentric factor ($\omega$) and molecular weight (Mw). The methods are artificial neural network (ANN) and adaptive network-based fuzzy inference System (ANFIS). A set of 159 data points (116, 23 and 20) was used for construct training, validating and testing, respectively. The radius parameter of ANFIS was determined through genetic algorithm (GA) optimization technique. The ANN and especially ANFIS results are in a good agreement with most of the compound groups.

Key words: Peng-Robinson-Stryjek-Vera Parameter, Artificial Neural Network, Adaptive Network-Based Fuzzy Inference System, Genetic Algorithm

## INTRODUCTION

Cubic equations of states (EOSs) are widely used in the many calculations of chemical and physical processes. The main usefulness of cubic EOS is their algebraic simplicity that makes them easy to use as well as needing only a small number of adjustable parameters which easily can be obtained from available physical properties. Despite much research in this field, there is a continued interest in improving the capability of estimating thermodynamic properties and phase equilibrium of pure and complex systems.

The Peng-Robinson (PR) EOS can represent both liquid and vapor behavior of non-polar molecules over limited range of temperature and pressure [1]. The PR EOS is accurate only for non polar compounds, while the PRSV-EOS [2] can reasonably estimate both polar and non polar compounds [2]. The PRSV EOS has an adjustable parameter, $\kappa_1$, which is determined using pure component vapor pressure experimental data [2]. Stryjek and Vera [2,3] calculated the values of the adjustable parameter for many compounds of industrial interest. The main disadvantage of PRSV-EOS is the determination of $\kappa_1$, which requires vapor pressure experimental data [2,3]. This problem arises when we know the vapor pressure data for many of compounds, especially for pseudo component materials which are extracted from herbaceous materials, and are not available in the literature. Therefore, a correlation should be obtained between the PRSV parameter with some relative thermodynamics parameters to estimate the parameter for every component without the need for vapor pressure data. However, there is not any correlation for this purpose. This reveals that there is a complicated relation between the dependent parameters ($\kappa_1$) with the independent parameters (thermophysical properties). In the present study, two models have been proposed using both ANN and ANFIS, as black boxes, in order to overcome this problem.

The ANN is a method for data processing of a huge number of simple highly interconnected processing elements in an architecture inspired by the structure of the brain [4]. Articial neural networks (ANNs) have been shown to be extremely suited to model highly complex and nonlinear phenomena. Owing to their inherent nature to model and learn 'complexities', ANNs have found wide applications in various areas of chemical engineering [5]. Hussain et al. [6] predicted the solubility of $CO_2$ in single monoethanolamine and diethanolamine solutions by a model developed based on the Kent-Eisenberg model in combination with a neural network. Park et al. [7] employed three black-box modeling techniques (support vector regression, partial least squares and ANN) to forecast heat consumption in the Suseo district heating network which is interconnected with other capital regional district heating networks. Zhang et al. [8] developed an empirical model to predict the boiler efficiency and pollutant emissions with ANN based on the experimental data on a 360 MW W-flame coal fired boiler. The ANN is also more applicable in estimation of properties and thermodynamic behavior of solution. An accurate neural network to estimate the supercritical extraction from Anise seed was presented by Shokri et al. [9]. Zahedi et al. [10] applied a combination of artificial neural network and fuzzy logic for modeling of yield of nimbin extraction from neem seeds using supercritical carbon dioxide with methanol as co-solvent. Their model was in excellent agreement with experimental data. Godini et al. [11] developed an experimental based artificial neural network model to describe the dialysis process performance under different operating conditions in the charged and neutral states of dialysis. Shokrian et al. [12] developed an MLP neural network model in order to predict separation factor (SF) of $C_3H_8$ during membrane GS process using a rubbery PDMS membrane. For almost all the experiments, the ANN was confirmed to

†To whom correspondence should be addressed.
E-mail: masoudrahimi@yahoo.com

be an adequate interpolation tool, where good prediction was obtained. In another study, Safamirzaei et al. [13] expanded the ANN technique for modeling of the Henry's law constant as a function of temperature and salt concentration. Various concentrations of methyl ketones in aqueous sodium sulfate were employed in their work. Nguyen et al. [14] used an ANN model to estimate vapor-liquid equilibrium data for ternary systems saturated with salt.

The main objective of this study is to predict the PRSV parameter as a function of compound properties using ANN and ANFIS. These artificial intelligence methods could estimate the EOS parameter more accurately than the classical method, and continuing these methods for estimating all parameters of EOSs, especially for binary parameters, could decrease the EOS error in the estimating of the composition of mixture at equilibrium especially close to the critical point where cubic EOSs have failed. In the present work, the estimated $\kappa_1$ from ANN and ANFIS has been compared with the experimental data. In addition, in order to find acceptable estimated $\kappa_1$ values, the percent of average absolute deviations in vapor pressure has been used as a criterion.

## MATERIALS AND METHODS

In this part of the paper, first a conceptual discussion about the necessary thermodynamical properties for determining PRSV parameter is given. Then, the two black box modeling methods, ANN and ANFIS, are briefly described. In addition, the GA technique, which is used for determining of an adjustable parameter in ANFIS, is explained. Finally, three accepted statistical parameters, RMSE, $R^2$ and $Q^2$, are explained to show the accuracy of the models.

### 1. Thermodynamical Properties for Determining PRSV Parameter

$\kappa_1$ is a parameter of the PRSV equation of state, and it is specific for each chemical compound. Stryjek and Vera [2,3] reported the values of $\kappa_1$ for many compounds of industrial interest (one value of k1 for each compound). So, if we specify a compound, we can determine the value of $k_1$. Some usual thermodynamic properties used for specification of a chemical compound are critical temperature, critical pressure, critical molar volume, normal boiling point, molar volume at the normal boiling point, molecular weight and acentric factor.

Critical molar volume can be calculated using the value of critical temperature and critical pressure by the following correlation [1]:

$$V_c = \frac{Z_c R T_c}{P_c} \quad (1)$$

Where R is the universal gas constant and $Z_c$ is the critical compressibility factor that can be obtained from equation of states.

Normal boiling point has a relation with critical temperature and molecular weight through a simple correlation [15]. Also, Tyn and Calus [16] obtained a power relation between critical molar volume and molar volume at the normal boiling point. So, from the mentioned thermodynamic properties, we chose critical temperature, critical pressure, molecular weight and acentric factor as the independent properties that can be used for specification of a chemical compounds. In other words, $\kappa_1$ is a function of these four thermodynamic properties.

### 2. ANN Model

ANN is parallel computational procedure consisting of highly interconnected processing elements groups named neurons. Neural networks are determined by training rules, computational characteristics of their elements and topology. Neural networks have several layers. The first layer is the input layer, and each of its neurons receives information corresponding to one of the independent variables used as inputs. The last layer is the output layer, and the other layers are called hidden layers, which are neurons between the input and output layers [17]. Neural networks may learn using two types of learning: supervised (both input and output information used for training) or unsupervised (only input information is available for training). As an example, probabilistic and backpropagation (BP) neural network use supervised learning, while most of the self-organizing neural networks are based on unsupervised learning [17]. Backpropagation neural network algorithm (BNN) has been used in this study as it is very fast and can be employed quite easily [18]. The training set should be used to adjust the parameters of the models, and testing set used to calculate its estimation power. The main problem in using neural networks is over-training probability. An over-trained network has typically learned the seen training set completely but cannot give accurate estimation for the unseen data. As a result, due to inaccurate data estimation, it cannot be able to be generalized. There are several techniques for avoiding this problem. One of the superior methods is using of a test set to validate the estimation ability of the network [19]. One of the most important factors in a neural network model configuration is to determine the number of layers to be used and the number of neurons in the layers. The number of input and output neurons is equal to the number of input and output parameters, respectively. The number of hidden layers and nodes is usually determined via a trial and error procedure. There are some rules to estimate the number of hidden nodes. According to the method suggested by Anderson and McNeill [20], an upper bound for the number processing nodes in the hidden layers can be calculated by dividing the number of input-output pairs in the training set by the total number of input and output nodes in the network multiplied by a scaling factor between 5 and 10. About determination of weights and biases, the available data is divided into three sets: training, validation, and test. The error in the validation set is monitored during the training. The validation error usually decreases during the initial phase of training, as does the training set error. However, when the network begins to overfit the data, the error on the validation set begins to rise. When the validation error increases for a number of iterations, the training is stopped, and the weights and biases at the minimum of the validation error are returned.

### 3. ANFIS

The structural design and learning rule of ANFIS have been described in Ref. [21] in detail. ANFIS is a multilayer feedforward network where each node performs a particular function on incoming signals [22,23]. To perform desired input/output characteristics, adaptive learning parameters are updated based on gradient learning rules [21]. The ANFIS model is one of the implementation of a first-order Sugeno fuzzy inference system [24]. Use of the clustering information to generate a Sugeno-type fuzzy inference system recently has been accelerated [25,26]. It models the data set behavior with a minimum number of rules. The rules divide themselves according to the fuzzy qualities associated with each of the data clusters. The number of clusters or optimum radius of clusters in

a purpose cluster pattern is the most important parameter in clustering. In general, clustering is for identification natural groupings of data from a large data set to produce a brief representation of a system's behavior [26].

**4. GA**

Genetic algorithms are search procedures based on the mechanics of natural genetic and natural selection [4]. In the present study, GA is applied to determine the optimum radius of clustering in each input/output data which minimize the difference between $\kappa_1$ estimation of the models and experimental data. The genetic operators have been developed to enhance the searching ability of GA. These operators are crossover, selection and three mutation operators consisting of inverse-anticdon, maximum-minimum, and normal-mutation [27]. Choosing methods and parameters in GA might result in very different results. An excellent configuration may cause the algorithm to converge to the best results in a small amount of time, while a worse setting might cause the algorithm to run for a long time before finding a good solution or it even might never be able to find a good solution. There are many parameters that affect the GA performance, such as population size, generations, mutation method, recombination method, parent selection method and so on. To be able to compare the effect of changing each parameter on genetic algorithm results we needed to fix all parameters except one of them. Subsequently, we changed that parameter and plotted the fitness function. The GA parameters were set to obtain the best performance and minimum runtime via this procedure and based on our previous experience.

**5. Statistical Parameters**

Three accepted statistical parameters were used to show the accuracy of the models. The first one is the RMSE [28]:

$$\mathrm{RMSE}=\sqrt{\frac{\sum_{i=1}^{N}\left(\kappa_{1,i}^{exp}-\kappa_{1,i}^{pre}\right)^2}{\mathrm{N}}} \tag{2}$$

Where $\kappa_{1,i}^{exp}$ and $\kappa_{1,i}^{pre}$ are the experiment and predicted $\kappa_1$ value of component i, respectively. In addition, N is the number of employed data. The second criterion is $R^2$ values which is a measure of goodness of the predictions. The $R^2$ values of the models are calculated as follows [19]:

$$\mathrm{R}^2=\frac{\left(\sum_{i=1}^{N}\{(\kappa_{1,i}^{exp}-\kappa_{1,mean}^{exp})(\kappa_{1,i}^{pre}-\kappa_{1,mean}^{pre})\}\right)^2}{\sum_{i=1}^{N}\left(\kappa_{1,i}^{exp}-\kappa_{1,mean}^{exp}\right)^2\sum_{i=1}^{N}\left(\kappa_{1,i}^{pre}-\kappa_{1,mean}^{pre}\right)^2} \tag{3}$$

In which, $\kappa_{1,mean}^{exp}$ and $\kappa_{1,mean}^{pre}$ are averages of experiment and predicted of $\kappa_1$, respectively. The third criterion is the $Q^2$ value that measures the goodness of the predictions of the held out cases exactly in the same way as $R^2$ does, but $Q^2$ is always lower and may be even negative if the predictions are worse than just using the average value of the response. The $Q^2$ value should be at least 0.3-0.4 in order to assess that the model has statistically significant prediction ability. The $Q^2$ value of the models is defined as follows [28]:

$$\mathrm{Q}^2=1-\frac{\sum_{i=1}^{N}\left(\kappa_{1,i}^{exp}-\kappa_{1,mean}^{pre}\right)^2}{\sum_{i=1}^{N}\left(\kappa_{1,i}^{exp}-\kappa_{1,mean}^{pre}\right)^2} \tag{4}$$

**6. Data Set**

The PRSV parameter of the whole 159 industrial compounds of interest, which previously were determined [2,3], has been used as a data set in the present study. The minimum and maximum values of the data set are 126.2 K to 774.7 K for critical temperature, 1215.89 kPa to 22089.75 kPa for critical pressure, 0.01045 to 0.79278 for acentric factor, 16.043 to 254.5 for molecular weight and −0.42503 to 0.8294 for PRSV parameter. For ANN and ANFIS, the 116, 23 and 20 of whole 159 compounds were used to construct training, validation and testing sets, respectively. The selection of all datasets has been done using a random method. From numerous available experimental data sets, ones which consider the distribution of compounds belonging to a different chemical group such as alcohol, ether and so on, have been selected. This has been done in order to consider the embrace of the data either in training, validation or test. Finally, the minimum error has been used as a criterion to determine the best dataset.

## RESULTS AND DISCUSSIONS

Network structure has a significant effect on the predicted results. To obtain more accurate ANN results, the parameters that influence the performance such as transfer function, number of hidden layers, number of hidden layer's neuron and learning rate were optimized. These parameters are usually determined via a trial and error procedure. In this study, numerous combinations of network geometry, from one hidden layer to three hidden layers, as well as various values for learning rate, from 0.05 to 0.9, were experimented. For each number of hidden layers and the values of learning rate, various numbers of nodes for each hidden layer were examined systematically. Also, different kinds of transfer functions were tested including hardlim, tansig, logsig, poslin, satlin and purelin. The network geometry which has the highest correlation and the lowest RMSE error of the testing and validation data sets is considered as the best network. The best neural network result has been obtained with one hidden layer network, with 13 neurons and 0.250 learning rate. Tansig for both hidden layer and output layer gave the best performance compared to other transfer functions. Once the network has been trained, the weights of each neuron are saved in the ANN model and are used to estimate the formation constant for unknown compounds. The (4-13-1) ANN, shown in Fig. 2, is trained

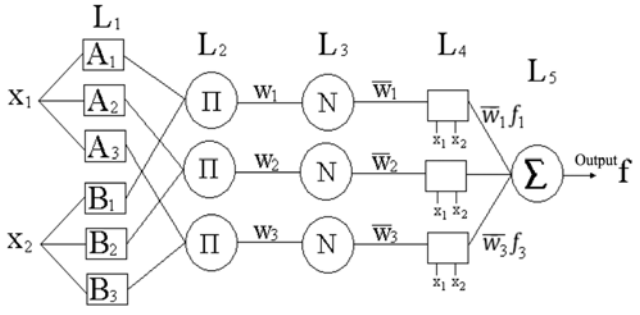


**Fig. 1. The ANFIS architecture with two inputs; $x_1$, $x_2$ one output f and three rules. Circles are the fixed nodes, squares are the adaptive nodes and A and B are the linguistic variables of the models.**

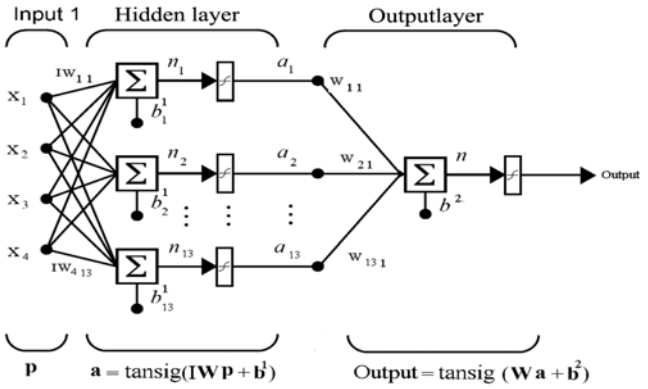


**Fig. 2. The architecture of (4-13-1) backpropagation ANN.**

with 116 dataset by the back propagation algorithm. The 79 fitting parameters, which determine the employed ANN in the present study, are listed in Table 1.

Turning to ANFIS, the function "genfis2" was applied to generate a first-order Sugeno-FIS, using subtractive clustering of the employed data set. Optimum radiuses which were obtained using GA are 0.1246, 0.0764, 0.0798, 0.0998 and 0.0125 for normalized value of Mw, $\omega$, Pc, Tc and $\kappa_1$, respectively. In addition, the 112 fuzzy rules were automatically generated by the application of "genfis2" using the optimum clustering radiuses.

The compound clustering is a meaningful way if and only if the values (e.g., critical properties, etc.) are of the same order of magnitude. From the presented data set, it is clear that there are a few compounds from the 116 training compounds which are placed in this category. This indicates that no clustering occurs in the data set, which completely agrees with the clustering results. The parameters associated with the initial membership functions are adjusted through the learning ANFIS process by applying a combination of the back propagation gradient decent method and the least squares method.

**Table 2. Statistical property of constructed ANFIS model**

| Modeling approach | Statistical parameter | Data set | | |
|---|---|---|---|---|
| | | Training set | Validation set | Test set |
| ANFIS | RMSE | $1.16\times10^{-4}$ | $5.65\times10^{-2}$ | $2.94\times10^{-2}$ |
| | $R^2$ | 1 | 0.72 | 0.89 |
| | $Q^2$ | 1 | 0.70 | 0.87 |
| ANN | RMSE | $2.65\times10^{-2}$ | $5.44\times10^{-2}$ | $7.10\times10^{-2}$ |
| | $R^2$ | 0.96 | 0.73 | 0.51 |
| | $Q^2$ | 0.96 | 0.73 | 0.26 |

Operators used automatically in tuning Sugeno fuzzy system are: AND method is product (prod), OR method is probabilistic OR (probor), defuzzification method is weighted average (wtaver), implication method is product, and aggregation method is maximum. The membership functions (MF) of the inputs were characterized as Gaussian MFs, and MFs of the outputs were specified as linear. The data set that was used for ANFIS modeling is the same as the data used for ANN modeling. Similar to ANN, the separate data sets, not included in the training set, were employed for validation and testing the ANFIS model generalization capabilities.

A summary of the statistical comparisons of ANFIS and ANN is given in Table 2. For a training data set that contains about 70% of the whole data set, $R^2$ and $Q^2$ are both unity for ANFIS model. The values of these parameters are 0.96 based on ANN model. For a validation data set that contains about 15% of the whole data set, ANN results are a little better than ANFIS results. For test data set, ANFIS results are also more accurate than ANN results. So, based on information presented in this table, it appears that the present ANFIS model is superior for estimating $\kappa_1$. About the meaningfulness of the comparison between the ANN and ANFIS models, it should to be noted that the authors allowed the ANN and ANFIS to find the best structure with optimum parameters (changing learning

**Table 1. (4-13-1) ANN parameters**

| Hidden layer parameters | | | | | | Output layer parameters | |
|---|---|---|---|---|---|---|---|
| | | | | | | $b^2$ | −2.8278 |
| IW | | | | | | W | |
| Neuron | Mw | w | Pc (kpa) | Tc (k) | $b^1$ | Neuron | Weight |
| 1 | −5.4044 | 7.7351 | −1.6832 | −10.3549 | 8.3375 | 1 | 8.6107 |
| 2 | 0.18792 | 4.1387 | −2.372 | −6.8483 | 5.6382 | 2 | −2.0268 |
| 3 | 4.7458 | −8.7516 | 3.8451 | 1.7837 | 5.6754 | 3 | −4.3993 |
| 4 | 1.9945 | 5.4106 | 5.1559 | 3.8183 | −0.6286 | 4 | −4.1235 |
| 5 | −0.54895 | −0.74623 | −5.0134 | −1.0593 | −0.85891 | 5 | 3.421 |
| 6 | 0.74018 | −0.43743 | −2.88 | 2.7263 | 2.7781 | 6 | 0.3357 |
| 7 | 1.1871 | 5.6006 | 3.5594 | 6.2351 | −3.516 | 7 | 3.7853 |
| 8 | 3.6191 | −7.2412 | −0.21899 | 0.67085 | 2.5979 | 8 | 7.873 |
| 9 | 5.5529 | −3.6441 | −4.1768 | 2.1242 | 2.5559 | 9 | −0.3295 |
| 10 | 1.9108 | 3.6778 | −3.6092 | 8.2978 | 0.85767 | 10 | −1.1299 |
| 11 | 3.5879 | −8.1594 | −4.0378 | −0.13127 | 0.70377 | 11 | −3.8544 |
| 12 | −1.998 | −5.0466 | 3.2441 | −7.9994 | −1.8908 | 12 | −1.1618 |
| 13 | −5.5265 | 11.287 | 4.8796 | −11.9999 | 15.1687 | 13 | −7.4027 |

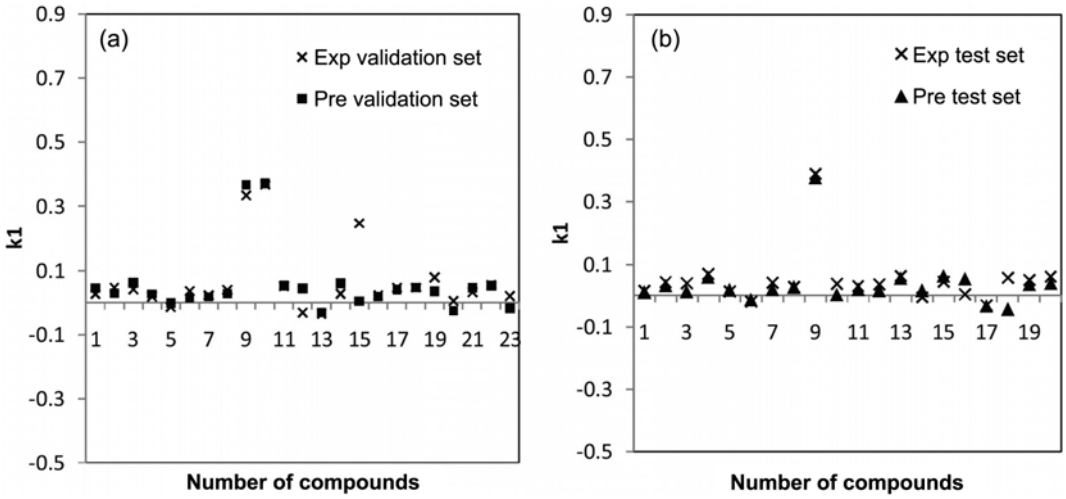


**Fig. 3. Comparisons between experimental and ANFIS results values of $\kappa_1$ for (a) validating (b) testing data.**

rate, the number of layer and number of neurons for ANN, changing the clustering radius for ANFIS). This leads to the optimum structure for both ANN and ANFIS. The difference between fitting parameter number of ANN and ANFIS is due to the basic difference of these methods. In addition, it was mentioned in the last paragraph of the introduction that the main objective of this study is to predict the PRSV parameter as a function of compound properties using the best model. For the above reasons, the comparison between the best models of ANN and ANFIS seems to be quite logical.

The fact that the prediction error is 0 for 103 of the data points in the training set is an inherent characteristic of ANFIS. In other words, the fuzzy algorithm detects them as centers of the clusters and thus defines the error associated with these points as zero. The validating and testing data sets showed reasonable agreement with experimental data, as shown in Fig. 3(a) and (b).

From thermodynamics point of view, it is not quite clear in which order the error is acceptable in determination of $\kappa_1$. Therefore, the percent of average absolute deviations (AADP%) in vapor pressure has been used as criterion to find an acceptable $\kappa_1$. For this purpose, the experimental and estimated PRSV parameter values have been used for calculating vapor pressure of each component reported by Stryjek and Vera [2] and Proust and Vera [3]. The employed temperature ranges are the same as those reported in the above-mentioned studies [2,3]. The AADP% is defined as follows and reported in Table 3 for each component.

$$\mathrm{AADP\%} = \frac{1}{\mathrm{N}}\sum_{i=1}^{N}\left|\frac{\mathrm{P}_i^{exp} - \mathrm{P}_i^{pre}}{\mathrm{P}_i^{exp}}\right| \times 100 \tag{5}$$

**Table 3. Comparison between the experimental values for with the obtained values from the ANN and ANFIS models and calculation of AADP% for each case**

| | | | ANN | | ANFIS | |
|---|---|---|---|---|---|---|
| Number | Components | Experimental | Prediction | AADP% | Prediction | AADP% |
| | | Train data set | | | | |
| 1 | Nitrogen | 0.01996 | 0.02249 | 0.02353 | 0.01996 | 0.00000 |
| 2 | Carbon dioxide | 0.04285 | 0.04529 | 0.02614 | 0.04285 | 0.00000 |
| 3 | Ammonia | 0.00100 | 0.00100 | 0.00002 | 0.00100 | 0.00000 |
| 4 | Water | −0.06635 | −0.06655 | 0.00241 | −0.06635 | 0.00000 |
| 5 | Hydrogen choloride | 0.01989 | 0.00755 | 0.14255 | 0.01989 | 0.00000 |
| 6 | Methane | −0.00159 | 0.02914 | 0.27600 | −0.00159 | 0.00000 |
| 7 | Propane | 0.03136 | 0.02014 | 0.11604 | 0.03136 | 0.00000 |
| 8 | Butane | 0.03443 | 0.05006 | 0.17450 | 0.03443 | 0.00000 |
| 9 | Neopentane | 0.04303 | 0.04030 | 0.02718 | 0.04303 | 0.00000 |
| 10 | Hexane | 0.05104 | 0.05490 | 0.03940 | 0.05104 | 0.00000 |
| 11 | Octane | 0.04464 | 0.05403 | 0.09854 | 0.04464 | 0.00000 |
| 12 | Decane | 0.04510 | 0.06450 | 0.28152 | 0.04510 | 0.00000 |
| 13 | Undecane | 0.02919 | 0.03642 | 0.03432 | 0.02919 | 0.00000 |
| 14 | Dodecane | 0.05426 | 0.04476 | 0.06108 | 0.05426 | 0.00000 |
| 15 | Tridecane | 0.04157 | 0.05838 | 0.14131 | 0.04157 | 0.00000 |

**Table 3. Continued**

| | | | ANN | | ANFIS | |
|---|---|---|---|---|---|---|
| Number | Components | Experimental | Prediction | AADP% | Prediction | AADP% |
| | | Train data set | | | | |
| 16 | Tetradecane | 0.02686 | 0.01141 | 0.15501 | 0.02686 | 0.00000 |
| 17 | Hexadecane | 0.02665 | 0.02679 | 0.00181 | 0.02665 | 0.00000 |
| 18 | Heptadecane | 0.04048 | 0.06114 | 0.28021 | 0.04048 | 0.00000 |
| 19 | Octadecane | 0.08291 | 0.06439 | 0.26396 | 0.08291 | 0.00000 |
| 20 | Cyclohegzane | 0.07023 | 0.05621 | 0.13438 | 0.07023 | 0.00000 |
| 21 | Bicyclohexyl | 0.01805 | 0.01819 | 0.00074 | 0.01805 | 0.00000 |
| 22 | Toluene | 0.03849 | 0.05057 | 0.12804 | 0.03849 | 0.00000 |
| 23 | Ethylbenzene | 0.03994 | 0.04910 | 0.10317 | 0.03993 | 0.00010 |
| 24 | Indene | 0.01173 | 0.02322 | 0.23103 | 0.01173 | 0.00000 |
| 25 | n-Propylbenzene | 0.02715 | 0.04254 | 0.15854 | 0.02715 | 0.00000 |
| 26 | Naphtalene | 0.03297 | 0.03592 | 0.06845 | 0.03297 | 0.00000 |
| 27 | 2-Methyl-naphtalene | −0.01639 | −0.02264 | 0.06911 | −0.01639 | 0.00000 |
| 28 | Biphenyl | 0.11487 | 0.11876 | 1.00247 | 0.11487 | 0.00000 |
| 29 | Diphenylmethane | 0.05955 | 0.05827 | 0.01504 | 0.05955 | 0.00000 |
| 30 | 9,10-Dihydrophenenthrene | −0.01393 | −0.01407 | 0.00180 | −0.01393 | 0.00000 |
| 31 | Acetone | −0.00888 | 0.00204 | 0.07016 | −0.00888 | 0.00000 |
| 32 | Butanone | 0.00554 | 0.01602 | 0.08614 | 0.00554 | 0.00000 |
| 33 | 2-Pentanone | 0.01681 | 0.02135 | 0.08703 | 0.01681 | 0.00000 |
| 34 | 2-Hexanone | 0.00984 | 0.00272 | 0.07262 | 0.00985 | 0.00000 |
| 35 | 5-Nonanone | 0.02002 | 0.01154 | 0.00163 | 0.02002 | 0.00000 |
| 36 | Methanol | −0.16816 | −0.16215 | 0.08253 | −0.16816 | 0.00000 |
| 37 | Ethanol | −0.03374 | −0.03877 | 0.07085 | −0.03374 | 0.00000 |
| 38 | 1-Propanol | 0.21419 | 0.21134 | 0.02970 | 0.21419 | 0.00000 |
| 39 | 2-Propanol | 0.23264 | 0.23414 | 0.00910 | 0.23264 | 0.00000 |
| 40 | 2-Methyl-1-propanol | 0.37200 | 0.37032 | 0.01339 | 0.37200 | 0.00000 |
| 41 | 2-Methyl-2-propanol | 0.43099 | 0.43540 | 0.01452 | 0.43099 | 0.00000 |
| 42 | 1-Hexanol | −0.00237 | 0.00192 | 0.01145 | −0.00237 | 0.00000 |
| 43 | 1-Octanol | 0.82940 | 0.81834 | 0.09235 | 0.82940 | 0.00000 |
| 44 | 1-Decanol | 0.80898 | 0.80754 | 0.02534 | 0.80898 | 0.00000 |
| 45 | Dimethyl ether | 0.05717 | 0.02148 | 0.17318 | 0.05717 | 0.00000 |
| 46 | Methyl ethyl ether | 0.16948 | 0.13282 | 0.42473 | 0.16948 | 0.00000 |
| 47 | Methyl n-propyl ether | 0.02300 | 0.05872 | 0.75518 | 0.02395 | 0.02013 |
| 48 | Methyl i-propyl ether | 0.04123 | 0.06732 | 0.53885 | 0.04065 | 0.01202 |
| 49 | Methyl n-butyl ether | 0.01622 | 0.04816 | 0.49551 | 0.01623 | 0.00000 |
| 50 | Ethyl n-propyl ether | −0.01668 | 0.04768 | 0.93643 | −0.01668 | 0.00000 |
| 51 | Methyl phenyl ether | 0.01610 | 0.01423 | 0.05400 | 0.01610 | 0.00000 |
| 52 | Nitromethane | −0.10299 | −0.12368 | 1.21410 | −0.10299 | 0.00000 |
| 53 | Acetonitrile | −0.13991 | −0.16626 | 0.30535 | −0.13991 | 0.00000 |
| 54 | Acetic acid | −0.19724 | −0.19681 | 0.00917 | −0.19724 | 0.00000 |
| 55 | Dimethylformamide | 0.18999 | 0.19867 | 1.12694 | 0.18999 | 0.00000 |
| 56 | 2-Methoxyethanol | −0.42503 | −0.39305 | 0.65907 | −0.42503 | 0.00000 |
| 57 | 1-Propylamine | 0.14326 | 0.03541 | 1.44546 | 0.14326 | 0.00000 |
| 58 | 2-Propylamine | 0.06001 | 0.04701 | 0.21094 | 0.06001 | 0.00000 |
| 59 | 2-Methoxypropionitrile | −0.09508 | −0.10197 | 0.19278 | −0.09508 | 0.00000 |
| 60 | 2-Methyl-2-propylamine | 0.13440 | 0.05507 | 0.70860 | 0.13388 | 0.00461 |
| 61 | Tetrahydrofuran | 0.03961 | 0.03998 | 0.00884 | 0.03961 | 0.00000 |
| 62 | Pyridine | 0.06946 | 0.07526 | 0.14427 | 0.06946 | 0.00000 |
| 63 | n-Methylpyrrolidone | 0.11367 | 0.10179 | 0.43624 | 0.11367 | 0.00000 |
| 64 | Nitrotoluene | −0.00901 | −0.00612 | 0.08573 | −0.00901 | 0.00000 |

**Table 3. Continued**

| | | | ANN | | ANFIS | |
|---|---|---|---|---|---|---|
| Number | Components | Experimental | Prediction | AADP% | Prediction | AADP% |
| | | Train data set | | | | |
| 65 | Thianaphthene | 0.06043 | 0.05911 | 0.01388 | 0.06043 | 0.00000 |
| 66 | Sulfur dioxide | 0.03962 | 0.03914 | 0.00478 | 0.03962 | 0.00000 |
| 67 | Carbon monoxide | 0.04279 | 0.02389 | 0.18874 | 0.04279 | 0.00000 |
| 68 | Acetylene | 0.09919 | 0.07225 | 0.27239 | 0.09919 | 0.00000 |
| 69 | Ethylene | 0.04191 | 0.02650 | 0.16448 | 0.04191 | 0.00000 |
| 70 | Isobutane | −0.00238 | 0.01860 | 0.21254 | −0.00238 | 0.00000 |
| 71 | 1,3-Butadiene | 0.02327 | 0.03491 | 0.02945 | 0.02328 | 0.00000 |
| 72 | Isopentane | 0.02840 | 0.06736 | 0.45947 | 0.02839 | 0.00016 |
| 73 | 1-Pentene | 0.03521 | 0.06742 | 0.31446 | 0.03527 | 0.00055 |
| 74 | 2,2,4-Trimethyl-pentane | 0.03363 | 0.05579 | 0.21639 | 0.03363 | 0.00000 |
| 75 | Methylcyclohexane | 0.04859 | 0.05954 | 0.26314 | 0.04859 | 0.00000 |
| 76 | o-Xylene | 0.02291 | 0.04585 | 0.26555 | 0.02293 | 0.00017 |
| 77 | m-Xylene | 0.01610 | 0.04328 | 0.27547 | 0.01610 | 0.00000 |
| 78 | i-Propylbenzene | 0.05509 | 0.05017 | 0.05231 | 0.05509 | 0.00000 |
| 79 | Styrene | 0.16109 | 0.15420 | 0.29893 | 0.16109 | 0.00000 |
| 80 | n-Butyric acid | −0.14012 | −0.15819 | 0.23479 | −0.14012 | 0.00000 |
| 81 | n-Valeric acid | −0.08171 | −0.07456 | 0.02282 | −0.08171 | 0.00000 |
| 82 | Propanal | −0.03642 | −0.00110 | 1.31719 | −0.03642 | 0.00000 |
| 83 | Ethyl formate | 0.11372 | 0.04043 | 0.81262 | 0.11373 | 0.00010 |
| 84 | Ethyl acetate | 0.06464 | 0.01353 | 0.60215 | 0.06464 | 0.00000 |
| 85 | n-Propyl acetate | 0.06531 | 0.02039 | 0.48972 | 0.06519 | 0.00135 |
| 86 | n-Butyl acetate | 0.07587 | 0.01799 | 1.06325 | 0.07587 | 0.00000 |
| 87 | Ethyl propionaate | 0.06362 | 0.01993 | 0.47696 | 0.06374 | 0.00128 |
| 88 | Diethyl ether | 0.05004 | 0.06282 | 0.13457 | 0.05016 | 0.00124 |
| 89 | Cyclohexanone | −0.29473 | −0.21762 | 1.39254 | −0.29473 | 0.00000 |
| 90 | Carbon tetrachloride | 0.05212 | 0.05231 | 0.00199 | 0.05212 | 0.00000 |
| 91 | Carbon tetraflouride | 0.02136 | 0.02171 | 0.00391 | 0.02136 | 0.00000 |
| 92 | Bromotrifluoromethane | 0.04014 | 0.03729 | 0.03183 | 0.04014 | 0.00000 |
| 93 | Trichlorofluoromethane | 0.03708 | 0.04901 | 0.13036 | 0.03708 | 0.00000 |
| 94 | Chloroform | 0.02899 | 0.01494 | 0.14944 | 0.02899 | 0.00000 |
| 95 | Chlorodifluoromethane | 0.04513 | 0.05253 | 0.08172 | 0.04513 | 0.00000 |
| 96 | Difluoromethane | −0.02874 | 0.00522 | 0.35143 | −0.02874 | 0.00000 |
| 97 | Methyl chloride | 0.01160 | −0.00265 | 0.14273 | 0.01160 | 0.00000 |
| 98 | Methyl fluoride | −0.00374 | 0.03709 | 0.38936 | −0.00374 | 0.00000 |
| 99 | 1,1-Trichloroethane | −0.00984 | 0.03610 | 5.57556 | −0.00984 | 0.00000 |
| 100 | 1,2-Trichloroethane | −0.04659 | 0.01069 | 2.75152 | −0.04659 | 0.00000 |
| 101 | Ethyl chloride | 0.03982 | 0.03829 | 0.01596 | 0.03982 | 0.00000 |
| 102 | Chlorobenzene | 0.03123 | 0.01348 | 0.18841 | 0.03123 | 0.00000 |
| 103 | Methylamine | 0.10475 | 0.10728 | 0.02910 | 0.10475 | 0.00000 |
| 104 | Ethylamine | 0.03536 | 0.06314 | 0.30897 | 0.03536 | 0.00000 |
| 105 | Dimethylamine | 0.20709 | 0.19538 | 0.11654 | 0.20709 | 0.00000 |
| 106 | Trimethylamine | 0.06414 | 0.04125 | 1.27210 | 0.06413 | 0.00052 |
| 107 | Diethylamine | 0.11210 | 0.04701 | 0.77740 | 0.11208 | 0.00026 |
| 108 | Triethylamine | 0.02951 | 0.05089 | 0.98716 | 0.02951 | 0.00000 |
| 109 | Aniline | 0.00316 | 0.00317 | 0.00005 | 0.00316 | 0.00000 |
| 110 | o-Toluidine | 0.03690 | 0.02266 | 0.35702 | 0.03690 | 0.00000 |
| 111 | m-Toluidine | 0.08293 | 0.09833 | 0.46165 | 0.08293 | 0.00000 |
| 112 | Ethylene oxide | 0.01757 | 0.02643 | 0.66521 | 0.01757 | 0.00000 |
| 113 | Propylene oxide | 0.03693 | 0.05916 | 0.22703 | 0.03693 | 0.00000 |

**Table 3. Continued**

| | | | ANN | | ANFIS | |
|---|---|---|---|---|---|---|
| Number | Components | Experimental | Prediction | AADP% | Prediction | AADP% |
| | | | Train data set | | | |
| 114 | o-Cresol | −0.00849 | −0.01179 | 0.09271 | −0.00849 | 0.00000 |
| 115 | p-Cresol | −0.04098 | −0.04027 | 0.01758 | −0.04098 | 0.00000 |
| 116 | Thiophene | 0.07654 | 0.05318 | 0.22789 | 0.07654 | 0.00000 |
| | | | Validation data set | | | |
| 1 | Ethane | 0.02669 | 0.02473 | 0.02162 | 0.04527 | 0.20504 |
| 2 | Heptane | 0.04648 | 0.05292 | 0.06860 | 0.02939 | 0.18183 |
| 3 | Nonane | 0.04104 | 0.05901 | 0.23990 | 0.06135 | 0.27119 |
| 4 | Pentadecane | 0.01892 | −0.01107 | 0.34075 | 0.02663 | 0.08795 |
| 5 | 1,2,3-Trimrthylbenzene | −0.01384 | 0.01838 | 0.33009 | −0.00127 | 0.12861 |
| 6 | 3-Pentanone | 0.03558 | 0.02313 | 0.26763 | 0.01491 | 0.44461 |
| 7 | 3-Hexanone | 0.02321 | 0.01773 | 0.08369 | 0.01781 | 0.08253 |
| 8 | Dimethylbutanone | 0.04005 | 0.04466 | 0.07489 | 0.02727 | 0.20838 |
| 9 | 1-Butanol | 0.33431 | 0.30636 | 0.23927 | 0.36728 | 0.28065 |
| 10 | 1-Pentanol | 0.36781 | 0.33011 | 0.56447 | 0.37204 | 0.06353 |
| 11 | Methyl t-butyl ether | 0.05129 | 0.05553 | 0.06426 | 0.05324 | 0.02958 |
| 12 | di-n-Propyle ether | −0.03162 | 0.04671 | 0.68651 | 0.04434 | 0.66607 |
| 13 | Furfural | −0.03471 | −0.06807 | 1.26093 | −0.03087 | 0.14371 |
| 14 | Hexafluorobenzene | 0.02752 | 0.03478 | 0.02922 | 0.05975 | 0.12834 |
| 15 | m-Cresol | 0.24705 | 0.15044 | 1.18144 | 0.00394 | 2.92774 |
| 16 | 1-Butane | 0.02222 | 0.03491 | 0.13171 | 0.01930 | 0.03027 |
| 17 | Cyclopentane | 0.04602 | 0.04907 | 0.03195 | 0.04121 | 0.05044 |
| 18 | Dichlorodifluoromethane | 0.04722 | 0.04931 | 0.02121 | 0.04728 | 0.00060 |
| 19 | Dichlorofluoromethane | 0.07915 | 0.07258 | 0.02400 | 0.03646 | 0.15944 |
| 20 | Trifluoromethane | 0.00535 | 0.02174 | 0.16078 | −0.02501 | 0.29669 |
| 21 | Chloropentafluoroethane | 0.03220 | 0.24195 | 2.32638 | 0.04606 | 0.15120 |
| 22 | 1,1,2-Trichlorotrifluoroethane | 0.05596 | 0.04707 | 0.10305 | 0.05298 | 0.03458 |
| 23 | Phenol | 0.02100 | −0.02398 | 1.76295 | −0.01786 | 1.52076 |
| | | | Test data set | | | |
| 1 | Oxigen | 0.01512 | 0.02100 | 0.05345 | 0.01178 | 0.03029 |
| 2 | Propene | 0.04400 | 0.02029 | 0.22082 | 0.03302 | 0.10238 |
| 3 | Pentane | 0.03946 | 0.06463 | 0.29603 | 0.01370 | 0.30154 |
| 4 | Benzene | 0.07019 | 0.05021 | 0.23081 | 0.06003 | 0.11750 |
| 5 | p-Xylene | 0.01277 | 0.04492 | 0.36090 | 0.01953 | 0.07569 |
| 6 | 1-Methyl-naphtalene | −0.01842 | 0.12159 | 0.26727 | −0.01230 | 0.01058 |
| 7 | Methylbutanone | 0.04113 | 0.03987 | 0.02815 | 0.02027 | 0.46757 |
| 8 | 2-Heptanone | 0.02731 | −0.00454 | 0.20789 | 0.02787 | 0.00362 |
| 9 | 2-Butanol | 0.39045 | 0.42229 | 0.22880 | 0.37675 | 0.09881 |
| 10 | di-I Propyl ether | 0.03751 | 0.05558 | 0.15476 | 0.00239 | 0.30411 |
| 11 | Hydrogen sulfide | 0.03160 | −0.06314 | 0.87624 | 0.02094 | 0.09947 |
| 12 | Cholorine | 0.03641 | −0.05743 | 0.92184 | 0.01707 | 0.19168 |
| 13 | Nitrous oxide | 0.06325 | 0.01892 | 0.43745 | 0.05663 | 0.06547 |
| 14 | 2-Methylpropene | −0.00516 | 0.04673 | 0.52704 | 0.01759 | 0.23051 |
| 15 | cis-2-Butene | 0.04457 | 0.05819 | 0.15273 | 0.06266 | 0.20300 |
| 16 | trans-2-Butene | 0.00435 | 0.08088 | 0.89267 | 0.05443 | 0.58267 |
| 17 | Propionic acid | −0.03093 | 0.18056 | 3.18447 | −0.03285 | 0.03020 |
| 18 | Methyl acetate | 0.05791 | 0.01143 | 0.50690 | −0.04230 | 1.08813 |
| 19 | Cholorotrifluoromethane | 0.05054 | 0.02208 | 0.27588 | 0.03643 | 0.13697 |
| 20 | 1,2-Dichlorotetrafluoroethane | 0.06095 | 0.06353 | 0.02832 | 0.04055 | 0.22356 |

**Table 4. AADP% distribution of validation and test for the applied modeling techniques (ANN and ANFIS)**

| | | ANN | ANFIS |
|---|---|---|---|
| Train | AADP%<1 | 91.38% | 100% |
| | max (AADP%) | 5.58 | 0.02 |
| Validation | AADP%<1 | 82.61% | 91.3% |
| | max (AADP%) | 2.33 | 2.93 |
| Test | AADP%<1 | 95% | 95% |
| | max (AADP%) | 3.18 | 1.09 |

In which P is pressure (MPa). The method for calculating $P^{prv}$ using the PRSV EOS is explained in Appendix A. To analyze the results, AADP% distribution of validation and test for the employed modeling technique (ANN and ANFIS) have been reported in Table 4. Especially, the percent of data with the AADP% lower than one percent is given in this table. Moreover, the maximum AADP% value has been determined and is shown in the table. For the most of estimated AADP% using ANFIS results, the error is lower than one percent. The maximum calculated AADP% for the ANN and ANFIS is 5.6 and 2.9, respectively. All these results indicate that ANFIS model could predict the PRSV parameter more efficiently in comparison with the ANN method.

To study the results more efficiently, the 159 compounds were divided into 15 chemical groups in Table 5. In each group, the average and maximum value of AADP% for each model have been calculated and, furthermore, the number of compounds, $N_C$, in each group has been determined. As can be seen from this table, the AADP% values of ANFIS model are lower than that of ANN model for all compounds with the exception of oxygen compounds. In the case of oxygen compounds, the average values of AADP% are 0.57 and 0.64 for ANN and ANFIS model, respectively. So, the ANFIS model has the best estimation for all compounds with exception of oxygen compounds. The best results for ANN and ANFIS have been obtained with alcohol and nitrogen compounds, respectively. However, calculation of the PRSV parameter using applied methods for the chemical groups with $N_C$<6 cannot be recommended.

**Table 5. AADP% for various groups of compounds using ANN and ANFIS**

| | | AADP% (ANN) | | AADP% (ANFIS) | |
|---|---|---|---|---|---|
| Chemical group | $N_C$[a] | Average | Max | Average | Max |
| Inorganic | 11 | 0.24 | 0.92 | 0.04 | 0.19 |
| Hydrocarbon | 52 | 0.21 | 1.00 | 0.05 | 0.58 |
| Keton | 13 | 0.31 | 1.39 | 0.10 | 0.47 |
| Alcohol | 13 | 0.16 | 0.66 | 0.03 | 0.28 |
| Ether | 11 | 0.40 | 0.94 | 0.09 | 0.67 |
| Acid | 4 | 0.86 | 3.18 | 0.01 | 0.03 |
| Aldehyd | 1 | 1.32 | 1.32 | 0.00 | 0.00 |
| Ester | 6 | 0.66 | 1.06 | 0.18 | 1.09 |
| Halogen compound | 21 | 0.61 | 5.58 | 0.05 | 0.30 |
| Nitrogen compound | 12 | 0.48 | 1.27 | 0.00 | 0.00 |
| Oxygen compound | 7 | 0.57 | 1.76 | 0.64 | 2.93 |
| Sulfur compound | 2 | 0.12 | 0.23 | 0.00 | 0.00 |
| Nitril | 2 | 0.25 | 0.31 | 0.00 | 0.00 |
| Amid | 1 | 1.13 | 1.13 | 0.00 | 0.00 |
| Amin | 3 | 0.79 | 1.45 | 0.00 | 0.00 |

[a]Number of compound

The PRSV EOS can be used for calculation of composition of multi-component mixtures in vapor liquid equilibrium systems, the density of liquids or vapors, and vapor pressure of pure liquid if and only if the PRSV parameter is available. So, prediction of the PRSV parameter by ANN or ANFIS and subsequently the hybrid of these artificial intelligence techniques with PRSV EOS can predict equilibrium composition of mixtures, pure fluid properties and vapor pressure of liquids. However, direct prediction of these thermophysical properties using ANN or ANFIS model needs several models for vapor pressure, fluid properties, and equilibrium composition. The other point is that unlike direct formulation of ANN or ANFIS model that needs too many experimental data of each specific compound for construction of the model, the proposed technique just needs the critical properties, acentric factor and molecular weight of the compound.

## CONCLUSION

A relationship between PRSV parameter, $\kappa_1$, and common thermodynamic constants of components, namely critical temperature, critical pressure, acentric factor and molecular weight, have been found by using the ANN and ANFIS modeling methods. The dataset was divided into three parts, including training set to adjust the parameters of the models, validation set to prevent the overtraining and testing set to test the model. Moreover, the radius parameter of the ANFIS method has been calculated using GA optimization technique. The results show that the ANFIS model gave the best estimations for all compounds except for oxygen compounds. For the oxygen compounds, the ANN gave more accurate estimations than those of ANFIS. Using these models, one can calculate the PRSV parameter of a pure or pseudo component without need for any vapor pressure data, and consequently, thermodynamic problems can be solved with PRSV EOS. The sensitivity analysis for ANFIS method revealed that 91.3 percent of the validation and 95 percent of test data set have AADP% lower than 1 percent. Furthermore, the maximum AADP% of ANFIS is 2.93 and 1.0 for validation and test data set, respectively.

## APPENDIX A. VAPOR PRESSURE CALCULATION METHOD

The main objective of this section is to describe the method for calculating the pure components vapor pressure through PRSV EOS.

At vapor-liquid equilibrium condition, the fugacity coefficient of vapor and liquid phase must be the same [29]:

$$\Phi^v = \Phi^l \tag{A.1}$$

Fugacity coefficient is calculated from the following equation [1]:

$$\Phi^i = \exp\left( (z^i - 1) - \mathrm{Ln}\left(z^i - \frac{bP}{RT}\right) - \frac{1}{2\sqrt{2}}\frac{a}{bRT}\mathrm{Ln}\left(\frac{z^i + (1+\sqrt{2})\frac{bP}{RT}}{z^i + (1-\sqrt{2})\frac{bP}{RT}}\right)\right) \tag{A.2}$$

Where superscript i can be vapor (v) or liquid ($l$), z is compressibility factor, P is pressure (MPa), T is temperature (K), R is the gas constant and a and b are the parameters of PRSV EOS. An equivalent form of the PRSV EOS is [1]:

$$z^3-\left(1-\frac{bP}{RT}\right)z^2+\left(\frac{aP}{R^2T^2}-3\left(\frac{bP}{RT}\right)^2-2\frac{bP}{RT}\right)z-\left(\frac{aP}{R^2T^2}\frac{bP}{RT}+\left(\frac{bP}{RT}\right)^2+\left(\frac{bP}{RT}\right)^3\right)=0 \quad (A.3)$$

Eqs. (A.2) and (A.3) have been used to calculate the component vapor pressure using the following procedure:

1- Read the temperature T.

2- Guess a value for $P^{sat}$ and set $P=P^{sat}$.

3- Calculate the compressibility factor through Eq. (A.3). Eq. (A.3) has three roots: either all real or one real and two complex conjugate roots. At three roots condition, the largest positive real root is taken as the vapor compressibility factor ($z^v$), while the smallest positive real root is taken as liquid compressibility factor ($z^l$). The other root is meaningless. Merely one phase exists when a single positive real root or three equal positive real roots are calculated from Eq. (A.3), go to step 2.

4- Calculate $\Phi^v$ and $\Phi^l$ using Eq. (A.2).

5- Calculate error using the following equation:

$$\text{error}=\frac{\left|\Phi^v-\Phi^l\right|}{\Phi^v} \quad (A.4)$$

6- Set $P=P\times(1+\text{error})$ and go to step 3.

7- Steps 3 to 6 should be repeated until error$<\delta$ ($\delta$ is an arbitrary infinitesimal number such as $10^{-12}$).

## ACKNOWLEDGEMENTS

The authors wish to express their thanks to Prof. J. H. Vera, Department of Chemical Engineering, McGill University, Montreal, Que., Canada H3A 2A7, for his experimental data of PRSV parameter.

## NOMENCLATURE

a ($Pa\cdot m^6\cdot kmol^{-2}$) : a parameter of PRSV EOS
AADP% (-) : the percent of average absolute deviations
b : a parameter of PRSV EOS [$m^3\cdot Kmol^{-1}$]
: bias of ANN model [-]
Mw ($kg\cdot Kmol^{-1}$) : molecular weight
N (-) : number
P (Pa) : pressure
$Q^2$ (-) : a statistical parameter
R ($J\cdot mol^{-1}\cdot K^{-1}$) : universal gas constant
$R^2$ (-) : correlation coefficient
RMSE (-) : root mean square error
T (K) : temperature
V ($m^3\cdot mol^{-1}$) : molar volume
w (-) : weights of ANN model
z (-) : compressibility factor

### Greek Letters

$\kappa_1$ (-) : PRSV parameter
$\Phi$ (-) : fugacity coefficient
$\omega$ (-) : acentric factor

### Subscripts

c : critical property
: compound

### Superscripts

exp : experimental
$l$ : liquid
pre : prediction
sat : saturation
v : vapor

## REFERENCES

1. R. C. Rpeid, J. M. Prausnitz and B. E. Poling, *The properties of gases and liquids*, 4th Ed., McGraw-Hill, New York (1987).
2. R. Stryjek and J. H. Vera, *Can. J. Chem. Eng.*, **64**, 323 (1986).
3. P. Proust and J. H. Vera, *Can. J. Chem. Eng.*, **67**, 170 (1989).
4. S. Rajasekaran and G. A. Vijayalakshmi-Pai, *Neural networks, fuzzy logic, and genetic algorithms*, Prentice-Hall, India (2007).
5. D. M. Himmelblau, *Korean J. Chem. Eng.*, **17**(4), 373 (2000).
6. M. A. Hussain, M. K. Aroua, C. Y. Yin, R. A. Rahman and N. A. Ramli, *Korean J. Chem. Eng.*, **27**, 1864 (2010).
7. T. C. Park, U. S. Kim, L. H. Kim, B. W. Jo and Y. K. Yeo, *Korean J. Chem. Eng.*, **27**, 1063 (2010).
8. Y. Zhang, Y. Ding, Z. Wu, L. Kong and T. Chou, *Korean J. Chem. Eng.*, **24**, 1118 (2007).
9. A. Shokri, T. Hatami and M. Khamforoush, *J. Supercrit. Fluids*, **58**, 49 (2011).
10. G. Zahedi, S. Azizi, T. Hatami and L. Sheikhattar, *The Open Chem. Eng. J.*, **4**, 21 (2010).
11. H. R. Godini, M. Ghadrdan, M. R. Omidkhah and S. S. Madaeni, *Desalination*, **265**, 11 (2011).
12. M. Shokrian, M. Sadrzadeh and T. Mohammadi, *J. Membr. Sci.*, **346**, 59 (2010).
13. M. Safamirzaei, H. Modarress and M. Mohsen-Nia, *Fluid Phase Equilib.*, **266**, 187 (2008).
14. V. D. Nguyen, R. R. Tan, Y. Brondial and T. Fuchino, *Fluid Phase Equilib.*, **254**, 188 (2007).
15. K. M. Klincewicz and R. C. Reid, *AIChE J.*, **30**, 137 (1984).
16. M. T. Tyn and W. F. Calus, *Processing*, **21**(4), 16 (1975).
17. M. T. Hagan, H. B. Demuth and M. Beale, *Neural Network Design*, PWS, Boston, MA (1996).
18. S. P. Niculescu, *J. Mol. Struct.*, **622**, 71 (2003).
19. MATLAB User's Guide (2007).
20. D. Anderson and G. McNeill, *Artificial neural networks technology*, Data&Analysis Center for Software (1992).
21. J. S. R. Jang, *IEEE International Conference on Syst. Man Cybernet.*, **23**, 665 (1993).
22. T. Takagi and M. Sugeno, *IEEE Trans. Syst. Man Cybernet.*, **15**, 116 (1985).
23. M. Sugeno and G. T. Kang, *Fuzzy Sets Syst.*, **28**, 15 (1998).
24. A. D. Kulkarni, *Computer vision and fuzzy neural systems*, Prentice-Hall, Englewood Cliffs, NJ (2001).
25. E. Entchev and L. Yang, *J. Power Sources*, **170**, 122 (2007).

26. A. Perendeci, S. Arslan, A. Tanyola and S. S. Çelebi, *Bioresour. Technol.*, **100**, 4579 (2009).
27. X. Chen and N. Wang, *Chem. Eng. J.*, **150**, 527 (2009).
28. E. Buyukbingol, A. Sisman, M. Akyildiz, F. N. Alparslan and A. Adejare, *Bioorg. Med. Chem.*, **15**, 4265 (2007).
29. J. M. Prausnitz, R. N. Lichtenthaler and E. G. D. Azevedo, *Molecular thermodynamics of fluid-phase equilibria*, 3th Ed., Prentice Hall, Englewood Cliffs, NJ (1999).